DISCUSSION

The epidemiological features of moyamoya disease have been reported several times in Japanese literature. [1-4] However, as shown in table 1, there are several differences in the epidemiological features of moyamoya disease between the data from previously and our study. The result shown in our study can not always exclude the latent regional bias although this bias seems to be small enough to neglect. However, in order to minimize this regional bias, the age and sex of this data obtained from Hokkaido were adjusted to those of the whole Japanese population. As far as the race/ethnicity is concerned, all data in this study was purely obtained from Japanese. The results revealed in this study of higher detection rate and prevalence, peak shift in detection rate from children to adults, and change in the type of clinical findings and higher familial occurrence reflect the epidemiological features of moyamoya disease at present.

These three results are discussed herewith.

Higher detection rate and prevalence

The higher figures of detection rate and prevalence of moyamoya disease disclosed in this study do not necessarily indicate that the values of these 2 important epidemiological parameters have actually increased. Indeed, the increase in the registered number of adult patients with moyamoya disease has resulted in an increase in the values of detection rate and prevalence. These higher figures than previous reports [2, 10] are supposed to reflect the availability of appropriate diagnostic tools and the brain check-up system extensively developed in Japan. On the contrary, this figure can be lower than reality since this system can register the fatal case due to moyamoya disease. In any case, the higher detection rate and prevalence revealed in this study reflects the actual features of moyamoya disease.

Peak shift from children to adults

One of the well-known specific features of moyamoya disease is its 2-peak pattern of age distribution and its higher incidence in childhood in Japan. This study also revealed a 2 peak pattern similar to that reported in previous papers.[1-4,9] This study, however, revealed that the higher peak observed in adult, particularly female

patients, is more prominent than in children. This result is similar to the data of Uchino et al. that is multi-race/ethnicity study in non-Asian country. [10] It is conceivable that this difference is caused by the method of data sampling. Most of the previous surveys were conducted by using questionnaires on the epidemiological features of moyamoya disease. This method was affected by sampling hospitals. Previous survey had an inclination to subject mainly university hospitals and public general hospitals. In this study, however, the certificated patients from similar large hospitals were 48.7% of all, within 15.4% from university hospitals. The other 51.3% patients were from numerous neurosurgical, neurological or pediatric specialized small hospital or clinic. The selection of hospitals might lead to an overestimation of the number of pediatric patients and an underestimation of the number of adult cases in past literature.

Changes in types of clinical findings and familial occurrence

Minor changes in the types of clinical findings, including an increase in hemorrhage onset, is not always remarkable since it simply reflects an increased number of adult moyamoya patients in this study. However, with regard to clinical findings, the most remarkable difference observed in this study was an increase in the number of asymptomatic moyamoya patients. These patients accounted for 18.0% of the total number of patients. The driving force for the elevated number of asymptomatic cases is believed to be the brain check-up system in Japan [5,6] and the knowledge of the familial occurrence of moyamoya disease. These factors were responsible for the identification of asymptomatic patients and indicate that many asymptomatic moyamoya patients have still not been identified. The familial occurrence rate is 15.4% in this study and was higher than that reported previously. [9, 11,12] This increase is also a reflection of the screening of the families with a history of moyamoya disease.

CONCLUSION

The detection rate, incidence and prevalence of the moyamoya disease are higher than previously reported. The 2-peak pattern was recognized as previously reported. However, the peak of detection rate in adult patients was higher than that in pediatric patients. In addition, it was revealed that asymptomatic moyamoya patients are not always rare in Japan.

Acknowledgements

This work was supported in part by a grant from the Research Committee on Spontaneous Occlusion of the Circle of Willis sponsored by the Ministry of Health and Welfare of Japan.

REFERENCES

1. **Suzuki J**, Kodama N. Moyamoya disease--a review. *Stroke*. 1983;**14**:104-109.
2. **Wakai K**, Tamakoshi A, Ikezaki K, *et al*. Epidemiological features of moyamoya disease in Japan: findings from a nationwide survey. *Clin Neurol Neurosurg*. 1997;**99**(Suppl.2):S1-S5.
3. **Ikezaki K**, Inamura T, Kawano T, *et al*. Clinical features of probable moyamoya disease in Japan. *Clin Neurol Neurosurg*. 1997;**99**(Suppl 2):S173-S177
4. **Fukui M**. Current state of study on moyamoya disease in Japan. *Surg Neurol*. 1997;**47**:138-143
5. **Nakagawa T**, Hashi K. The incidence and treatment of asymptomatic, unruptured cerebral aneurysms. *J Neurosurg*. 1994;**80**:217-223.
6. **Yoshimoto Y**, Wakai S. Cost-effectiveness analysis of screening for asymptomatic, unruptured intracranial aneurysms. A mathematical model. *Stroke*. 1999;**30**:1621-1627
7. **Ohno Y**, Kawamura T, Tamakoshi A, *et al*. Epidemiology of diseases of unknown etiology, specified as "intractable diseases". *J Epidemiol*. 1996;**6**(Suppl.):S87-S94.
8. **Fukui M**. Research Committee on Spontaneous Occlusion of the Circle of Willis (Moyamoya Disease) of the Ministry of Health and Welfare, Japan. Guidelines for the diagnosis and treatment of spontaneous occlusion of the circle of Willis (moyamoya' disease). *Clin Neurol Neurosurg*. 1997;**99**(Suppl.2):S238-S240.
9. **Fukui M**, Kono S, Sueishi K, *et al*. Moyamoya disease. *Neuropathology*. 2000;**20**(Suppl.):S61-S64.
10. **Uchino K**, Johnston SC, Becker KJ, *et al*. Moyamoya disease in Washington State and California. *Neurology*. 2005;**65**:956-958
11. **Nanba R**, Tada M, Kuroda S, *et al*. Sequence analysis and bioinformatics analysis of chromosome 17q25 in familial moyamoya disease. *Childs Nerv Syst*. 2005;**21**:62-68
12. **Nanba R**, Kuroda S, Tada M, *et al*. Clinical features of familial moyamoya disease. *Childs Nerv Syst*. 2006;**22**:258-262.

Table 1 Epidemiological features of Moyamoya disease

	Present Study	1997 [2]
Number of cases	267	1176
Detection Rate (per 100,000)	0.94	0.35
Prevalence (per 100,000)	10.5	3.16
Sex ratio (male:female)	1:2.2	1:1.8
Patients younger than 10 years old at onset (%)	15.1%	47.8%
Pattern of age distribution	2 peaks	2 peaks
Highest peak in age distribution (in years)	45-49	10-14
Second peak in age distribution (in years)	5-9	40-49
Patients with family history	15.4%	10.0%

FIGURE LEGENDS

Figure 1
Geographical location of Hokkaido (gray) in Japan.

Figure 2
Onset age distribution of Moyamoya disease.

Figure 3
Age distribution of disease pattern at onset.

Figure 4
Disease patterns of Moyamoya disease at onset.

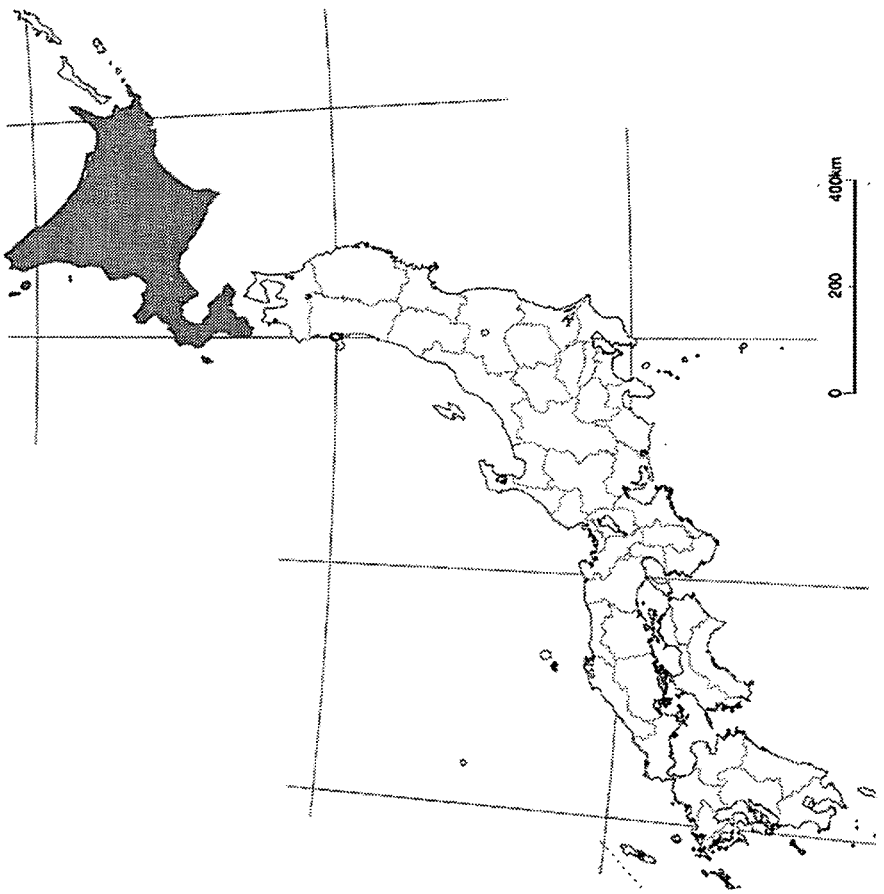
400km
200
0

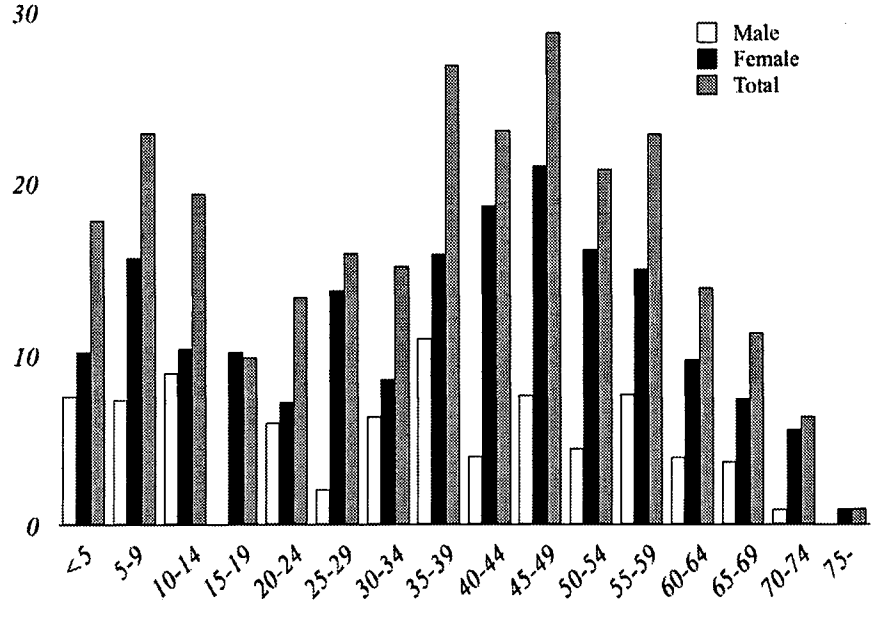
30
20
10
0
Male
Female
Total
<5
5-9
10-14
15-19
20-24
25-29
30-34
35-39
40-44
45-49
50-54
55-59
60-64
65-69
70-74
75-

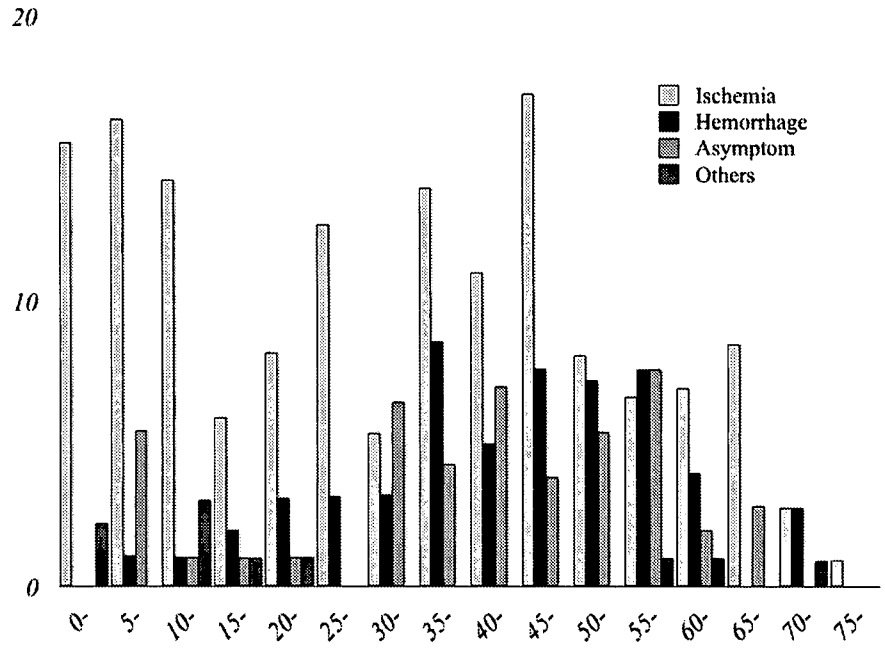
20
10
0
Ischemia
Hemorrhage
Asymptom
Others
0-
5-
10-
15-
20-
25-
30-
35-
40-
45-
50-
55-
60-
65-
70-
75-

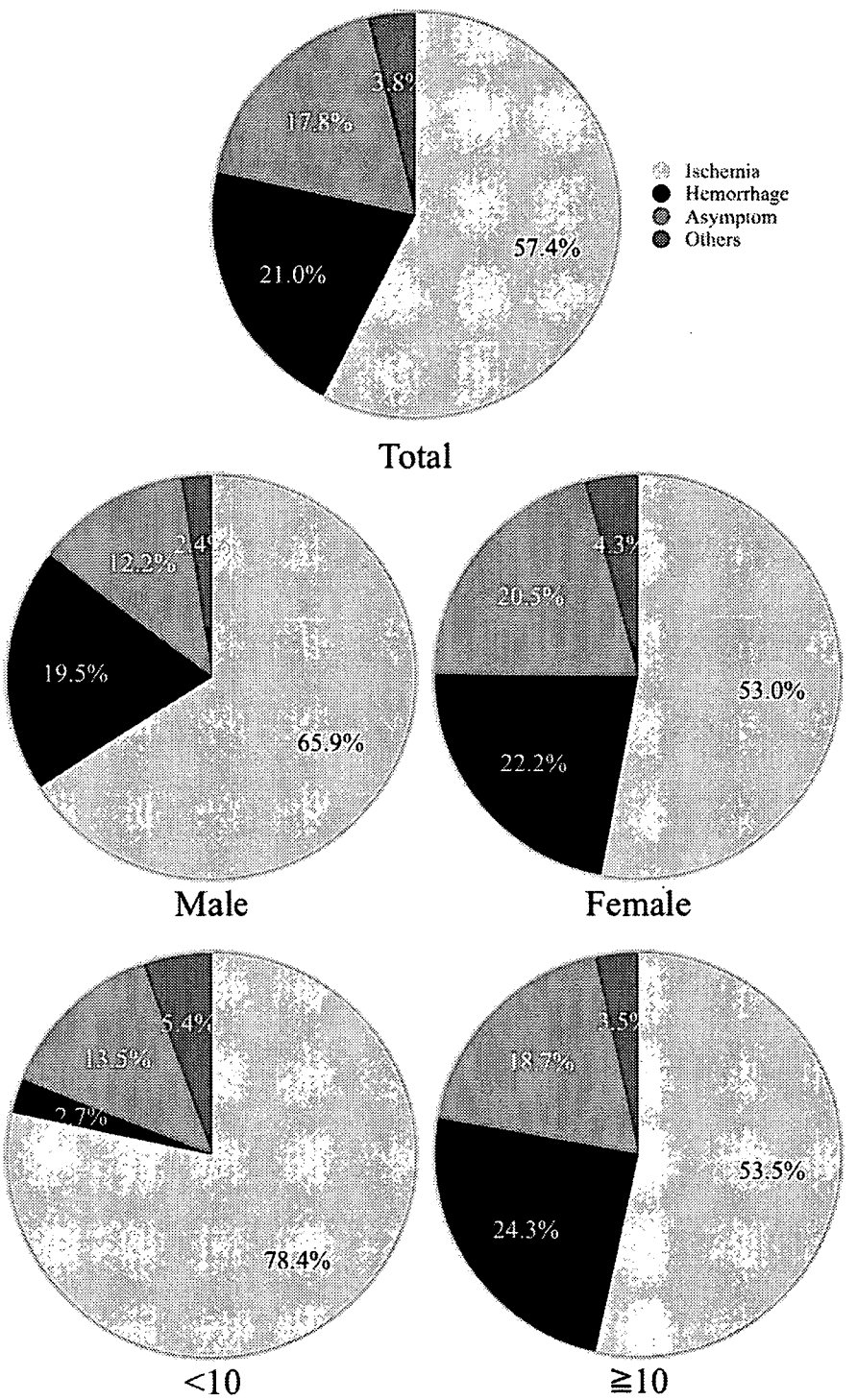
3.8%
17.8%
21.0%
57.4%
Ischemia
Hemorrhage
Asymptom
Others
Total
12.2%
2.4%
19.5%
65.9%
Male
20.5%
4.3%
53.0%
22.2%
Female
13.5%
5.4%
2.7%
78.4%
<10
18.7%
3.5%
24.3%
53.5%
≧10

Journal of Cerebral Blood Flow & Metabolism (2008) 28, 329–340

www.jcbfm.com

Therapeutic benefits by human mesenchymal stem cells (hMSCs) and Ang-1 gene-modified hMSCs after cerebral ischemia

Toshiyuki Onda[1], Osamu Honmou[1,3,4], Kuniaki Harada[1], Kiyohiro Houkin[1], Hirofumi Hamada[2] and Jeffery D Kocsis[3,4]

[1]*Department of Neurosurgery, Sapporo Medical University School of Medicine, Sapporo, Hokkaido, Japan;* [2]*Department of Molecular Medicine, Sapporo Medical University School of Medicine, Sapporo, Hokkaido, Japan;* [3]*Department of Neurology, Yale University School of Medicine, New Haven, Connecticut, USA;* [4]*Neuroscience Research Center, VA Medical Center, West Haven, Connecticut, USA*

Transplantation of human mesenchymal stem cells (hMSCs) prepared from adult bone marrow has been reported to ameliorate functional deficits after cerebral artery occlusion in rats. Although several hypotheses to account for these therapeutic effects have been suggested, current thinking is that both neuroprotection and angiogenesis are primarily responsible. In this study, we compared the effects of hMSCs and angiopoietin-1 gene-modified hMSCs (Ang-hMSCs) intravenously infused into rats 6 h after permanent middle cerebral artery occlusion. Magnetic resonance imaging and histologic analyses revealed that rats receiving hMSCs or Ang-hMSCs exhibited comparable reduction in gross lesion volume as compared with the control group. Although both cell types indeed improved angiogenesis near the border of the ischemic lesions, neovascularization and regional cerebral blood flow were greater in some border areas in Ang-hMSC group. Both hMSC- and Ang-hMSC-treated rats showed greater improved functional recovery in the treadmill stress test than did control rats, but the Ang-hMSC group was greater. These results indicate the intravenous administration of genetically modified hMSCs to express angiopoietin has a similar effect on reducing lesion volume as hMSCs, but the Ang-hMSC group showed enhanced regions of increased angiogenesis at the lesion border, and modest additional improvement in functional outcome.
Journal of Cerebral Blood Flow & Metabolism (2008) **28**, 329–340; doi:10.1038/sj.jcbfm.9600527; published online 18 July 2007

Keywords: angiogenesis; regeneration; stem and progenitor cells; stroke; transplantation

Introduction

Although transplantation of human mesenchymal stem cells (hMSCs) several hours after onset of ischemia can reduce infarction size and improve functional outcome in rodent cerebral ischemia models (Chen *et al*, 2001; Li *et al*, 2002; Iihoshi *et al*, 2004; Nomura *et al*, 2005; Honma *et al*, 2006; Horita *et al*, 2006; Liu *et al*, 2006), the detailed mechanisms by which MSCs promote functional recovery remain unclear. Angiogenesis is thought to be associated with improved neurologic recovery after ischemia (Krupinski *et al*, 1994; Chen *et al*, 2003).

Vascular endothelial growth factor has been reported to show strong angiogenetic effects in brain ischemia (Zhang and Chopp, 2002), limb ischemia (Baumgartner *et al*, 1998), and myocardial ischemia models (Kastrup, 2003). Vascular endothelial growth factor exerts its biologic functions via three related receptor tyrosine kinases, VEGFR-1, VEGFR-2, VEGFR-3 (Yancopoulos *et al*, 2000), and is required to initiate the formation of immature vessels by vasculogenesis or angiogenesis (Carmeliet and Collen, 1997). However, vascular endothelial growth factor (VEGF) is also a potent enhancer of vascular permeability to blood plasma proteins within minutes after ischemic insult, which often causes brain edema after the cerebral infarction (Wang *et al*, 1996; Bates *et al*, 2002).

Correspondence: Dr O Honmou, Department of Neurosurgery, Sapporo Medical University School of Medicine, South-1st, West-16th, Chuo-ku, Sapporo, Hokkaido 060-8543, Japan.
E-mail: honmou@sapmed.ac.jp
This work was supported in part by grants from the Japanese Ministry of Education, Science, Sports and Culture (16390414), Mitsui Sumitomo Insurance Welfare Foundation, the National Multiple Sclerosis Society (USA) (RG2135; CA1009A10), the National Institutes of Health (NS43432), and the Medical and Rehabilitation and Development Research Services of the Department of Veterans Affairs.
Received 13 February 2007; revised 20 May 2007; accepted 23 May 2007; published online 18 July 2007

Angiopoietin is involved in maturation, stabilization, and remodeling of vessels (Davis *et al*, 1996; Suri *et al*, 1996, 1998; Yancopoulos *et al*, 2000). Angiopoietin-1 is the best characterized member of this family and binds to Tie2, a receptor tyrosine kinase that is expressed on endothelial cells lining blood vessels and in the choroid plexus (Dumont *et al*, 1994; Nourhaghighi *et al*, 2003), and promotes angiogenesis in the brain (Ward and Lamanna, 2004). Furthermore, angiopoietin-1 (Ang-1) protects the peripheral vasculature from vascular leakage (Thurston *et al*, 1999), which may account for its anti-edematic effects after cerebral ischemia.

In the present study, hMSCs and Ang-1 gene-modified hMSCs (Ang-hMSCs), which had been transfected with the Ang-1 gene were intravenously delivered 6 h after induction of unilateral permanent cerebral ischemia to investigate if cellular delivery of Ang-1 by hMSCs could influence angiogenesis and functional outcome.

Materials and Methods

Preparation of Human Mesenchymal Stem Cells

Human mesenchymal stem cells were processed for cell culture as described previously (Nomura *et al*, 2005; Honma *et al*, 2006; Liu *et al*, 2006). Briefly, human bone marrow from healthy adult volunteers was obtained by aspiration from the posterior iliac crest after informed consent was obtained; the subject's consent was obtained according to the Declaration of Helsinki Principles, and this study was approved by the Institutional Review Board at our university. Bone marrow mononuclear cells were isolated, and were plated in 150-cm^2 plastic tissue culture flasks and incubated overnight. After washing away the free cells, the adherent cells were cultured in Mesenchymal Stem Cell Basal Medium (Cambrex, Walkersville, MD, USA) containing Mesenchymal Cell Growth Supplement (Cambrex), 4 mmol/L L-glutamine, in a humidified atmosphere of 5% CO_2 at 37°C. After reaching confluency, they were harvested and cryopreserved as primary MSCs or used for gene transduction.

Adenoviral Vectors

Adenoviral vectors carrying a human Ang-1 cDNA were constructed as described previously with minor modifications (Takahashi *et al*, 2003; Kurozumi *et al*, 2004). Briefly, human Ang-1 cDNA was cloned using the reverse transcription polymerase chain reaction method using the total RNA extracted from primary MSC as the template. The identity of Ang-1 cDNA obtained in this manner was confirmed by sequencing and comparing it with the GeneBank sequence U83508. The Ang-1 cDNA was inserted between the *Eco*RI site and the *Bgl*II site in the pCAcc vector, and the resulting plasmid was designated pCAhAng1. The plasmid pCAhAng1 was digested with *Cla*I, and the fragment containing the Ang-1 cDNA expression unit was isolated by agarose gel electrophoresis. The adenoviral Ang-1 expression vector, pWEAxCAhAng1-F/RGD, was prepared using LipofectAMINE 2000 (Invitrogen, Tokyo, Japan).

Before being used, the above viral vectors were evaluated for their viral concentration and titer, and viral stocks were examined for potential contamination with replication-competent viruses. To determine viral concentration (particle unit (pu)/mL), the viral solution was incubated in 0.1% sodium dodecyl sulfate and A_{260} was measured. The viral titers of AxCAhAng1-F/RGD were 1.0×10^{12} pu/mL, respectively.

Adenovirus Infection

Adenovirus-mediated gene transfection was performed as described previously (Takahashi *et al*, 2003; Kurozumi *et al*, 2004). Briefly, the cells were seeded at a density of 2×10^6 cells per 15 cm plate. Human mesenchymal stem cells were exposed to the infectious viral particles in 7.5 mL Dulbecco's modified Eagle's medium at 37°C medium for 60 mins; cells were infected with AxCAhAng1-F/RGD or AxCALacZ-F/RGD at an multiplicity of infection (MOI) of 3.0×10^3 pu/cell. The medium was then removed, and the cells were washed once with Dulbecco's modified Eagle's medium and then recultured with normal medium for 24 h, after which transplantation was performed.

Phenotypic Characterization of the Human Mesenchymal Stem and Angiopoietin-1 Gene-Modified Human Mesenchymal Stem Cells

Flow cytometric analysis of primary hMSCs and Ang-hMSCs were performed as described previously (Honma *et al*, 2006; Liu *et al*, 2006). Briefly, cell suspensions were washed twice with phosphate-buffered saline containing 0.1% bovine serum albumin. For direct assays, aliquots of cells at a concentration of 1×10^6 cells/mL were immunolabeled at 4°C for 30 mins with the following anti-human antibodies: fluorescein isothiocyanate (FITC)-conjugated CD45, CD34, CD105 (Immunotech, Marseilles, France), and anti-human CD73 (SH-3; BD Biosciences Pharmingen, San Diego, CA, USA). As an isotype-matched control, mouse immunoglobulin G1-FITC (IgG1-FITC; Immunotech) was used. Labeled cells were analyzed by a FACSCalibur flow cytometer (Becton Dickinson, Franklin Lakes, NJ, USA) with the use of CellQuest software. Dead cells were gated out with forward- versus side-scatter window and propidium iodide staining.

Cerebral Ischemic Model

The rat middle cerebral artery occlusion (MCAO) model was used as a stroke model. We induced permanent MCAO by using a previously described method of intraluminal vascular occlusion (Longa *et al*, 1989). Adult male Sprague–Dawley rats weighing 250 to 300 g were anesthetized with an intraperitoneal injection of ketamine (75 mg/kg) and xylazine (10 mg/kg). A length of 20.0 to

22.0 mm 4-0 surgical dermalon suture with the tip rounded by heating near a flame was advanced from the external carotid artery into the lumen of the internal carotid artery until it blocked the origin of the MCA.

Transplantation Procedures

Experiments consisted of three groups: group 1, medium (Mesenchymal Stem Cell Basal Medium) alone (without donor cell administration) ($n=32$); group 2, hMSCs (1.0×10^6) ($n=20$); and group 3, Ang-hMSCs (1.0×10^6) ($n=21$). All injections were made 6 h after MCAO and cells were suspended in 1 mL of medium.

In some experiments, AxCALacZ-F/RGD adenovirus was used to transduce the LacZ gene into the hMSC ($n=8$) and Ang-hMSC ($n=16$). For *in vitro* adenoviral infection, 1.0×10^7 MSCs were placed with AxCALacZ-F/RGD at a MOI of 3.0×10^3 pu/cell for 1 h and incubated at 37°C in medium containing 10% fetal calf serum.

Magnetic Resonance Imaging Studies and Measurement of Infarct Volume

Rats were anesthetized intraperitoneally with ketamine (75 mg/kg) and xylazine (10 mg/kg). Each rat was placed in an animal holder/magnetic resonance imaging (MRI) probe apparatus and positioned inside the magnet. The animal's head was held in place inside the imaging coil. All MRI measurements were performed using a 7-T, 18-cm-bore superconducting magnet (Oxford Magnet Technologies, Witney, Oxfordshire, UK) interfaced to a UNITYINOVA console (Oxford Instruments, UK and Varian, Palo Alto, CA, USA). T_2-weighted images (T_2WIs) were obtained from a 1.0-mm-thick coronal section with a 0.5 mm gap using a 30 mm × 30 mm field of view, TR = 3000 ms, TE = 37 ms, *b* value = 0, and reconstructed using a 256 × 256 image matrix. Diffusion-weighted images (DWIs) were obtained under the same condition as T_2WI except *b* value (1000). Accurate positioning of the brain was performed to center the image slice 5 mm posterior to the rhinal fissure with the head of the rat held in a flat skull position. Magnetic resonance imaging measurements were obtained 6, 24 h, 3, and 7 days after MCAO.

The ischemic lesion area was calculated from both T_2WI and DWI using imaging software (Scion Image, Version Beta 4.0.2, Scion Corporation, Frederick, MD, USA), based on the previously described method (Neumann-Haefelin *et al*, 2000). For each slice, the higher intensity lesions in both T_2WI and DWI, where the signal intensity was 1.25 times higher than the counterpart in the contralateral brain lesion, were marked as the ischemic lesion area, and infarct volume was calculated taking slice thickness (1 mm/slice) into account.

Detection of Angiopoietin-1 *In Vitro*

In separate dishes, we cultured hMSCs (1.0×10^5) transfected *in vitro* at various MOI (0, 300, 1000, and 3000 pu/cell). Forty-eight hours after hMSCs were transfected, culture supernatants were collected for analysis. The culture supernatants were centrifuged for 10 mins. Commercial Ang-1 ELISA kits (R&D Systems, Minneapolis, MN, USA) were used to quantify the concentration of Ang-1 in each of the samples.

2,3,5-Triphenyltetrazolium Chloride Staining and Quantitative Analysis of Infarct Volume

One week after transplantation, the rats were deeply anesthetized intraperitoneally with ketamine (4.4 to 8 mg/kg) and xylazine (1.3 mg/100 g). The brains were removed carefully and dissected into coronal 1 mm sections using a vibratome. The fresh brain slices were immersed in a 2% solution of 2,3,5-triphenyltetrazolium chloride (TTC) in normal saline at 37°C for 30 mins.

The cross-sectional area of infarction in each brain slice was examined with a dissection microscope and was measured using an image analysis software, NIH image. The total infarct volume for each brain was calculated by summation of the infarcted area of all brain slices.

Detection of Donor Angiopoietin-1 Human Mesenchymal Stem Cells *In Vivo*

X-gal Staining: One week after transplantation, the LacZ-transfected Ang-hMSCs *in vivo* were detected by X-gal staining. Brains of the deeply anesthetized rats were removed and fixed in 0.5% glutaraldehyde in phosphate buffer for 1 h. Brains were removed and brain slices (1000 μm) were cut with a vibratome, and β-galactosidase-expressing cells were detected by incubating the sections at 37°C overnight with X-gal to a final concentration of 1 mg/mL in X-Gal developer (35 mmol/L $K_3Fe(CN)_6$/35 mmol/L $K_4Fe(CN)_6 3H_2O$/2 mmol/L $MgCl_2$ in phosphate-buffered saline) to form a blue reaction product within the cell.

Immunohistochemistry

Two weeks after transplantation, the LacZ-transfected Ang-hMSCs *in vivo* were detected using laser-scanning confocal microscopy. Brains of the deeply anesthetized rats were removed, fixed in 4% paraformaldehyde in phosphate buffer, dehydrated with 30% sucrose in 0.1 mol/L phosphate-buffered saline for overnight, and frozen in powdered dry ice. Coronal cryostat sections (10 μm) were processed for immunohistochemistry. To identify the transplanted cells, LacZ-labeled Ang-hMSCs were visualized using the antibody to β-galactosidase (rhodamine-labeled polyclonal rabbit anti-β-galactosidase antibody, DAKO, Carpinteria, CA, USA). To identify the cell type derived from the donor Ang-hMSCs, double-labeling studies were performed with the use of antibody to endothelial cells (FITC-labeled polyclonal rabbit anti-von Willbrand factor (vWF); DAKO). To excite the FITC fluorochrome (green), a 488-nm laser line generated by an argon laser was used, and for the rhodamine fluorochrome

(red), a 543-nm laser line from a HeNe laser was used. Confocal images were obtained using a Zeiss laser-scanning confocal microscope with the use of Zeiss software.

Three-Dimensional Image Acquisition for Angiogenesis

Seven and twenty-eight days after MCAO, rats were anesthetized and intravenously perfused with FITC-dextran (1 mL, Sigma). The brains were immediately removed, and were fixed in 4% paraformaldehyde at 4°C for 48 h. Coronal vibratome sections (100 μm) were analyzed with a laser-scanning confocal imaging system (LSM Pascal; Carl Zeiss, Jend, Germany). The sections were scanned in 512 × 512 pixel (651.5 μm × 651.5 μm) format in the *x–y* direction using a 5 × frame-scan average (2.18 μm interval and 2.4 μm thickness along the *z* axis) under a × 20 objective. Vessel volumes were measured in three dimensions using the Zeiss LSM software.

Dynamic Susceptibility Contrast-Enhanced Perfusion-Weighted Imaging

Perfusion-weighted imaging was acquired using T_2^*-weighted (TR = 13 ms, TE = 6.0 ms) gradient echo sequence (Ukai *et al*, 2007). A dynamic image series of 30 measurements resulted in a total scan time of 26 secs, with a fields of view of 30 mm and image acquisition matrix of 128 × 64, which was interpolated by zero-filling to 512 × 512. During the dynamic series, a triple-dose (0.6 mL/kg) bolus injection of Magnevist (Schering AG, Berlin, Germany) was started after the fifth acquired volume to ensure a sufficient precontrast baseline. Images were reconstructed by an Inova Vision. Perfusion-weighted imaging measurements were obtained 6 h, 3, and 7 days after MCAO. For the perfusion-weighted imaging (PWI) and PWI-derived parameter maps, only one representative slice (involving cortex and stria terminalis) with the maximum lesion involving both cortex and striatum was chosen for cerebral blood flow quantification. The readout of abnormal regional cerebral blood flow (rCBF) from the regions of perfusion deficiency as a percentage of that measured in the contralateral brain was generated using Perfusion Solver software. Regions of interest (ROI) consists of four groups, based on the results of DWI, T_2WI, and PWI. ROI-1 is defined as abnormal in all images, ROI-2 as normal in only T_2WI and abnormal in others, ROI-3 as abnormal in only PWI and normal in others, and ROI-4 as normal in all images.

Treadmill Stress Test

Rats were trained 20 mins/day for 2 days a week to run on a motor-driven treadmill at a speed of 20 m/min with a slope of 0°C. Rats were placed on a moving belt facing away from the electrified grid and induced to run in the direction opposite to the movement of the belt. Thus, to avoid foot shocks (with intensity in 1.0 mA), the rats had to move forward. Only the rats that had learned to avoid the mild electrical shock were included in this study. The maximum speed at which the rats could run on a motor-driven treadmill was recorded.

Statistical Analysis

Data are presented as mean values ± s.d., and were statistically analyzed. Differences among groups were assessed by ANOVA with Scheffes *post hoc* test and the Kruskal–Wallis test to identify individual group differences. Differences were deemed statistically significant at $P < 0.05$.

Results

Characteristics of Primary and Angiopoietin-1 Gene-Transduced Human Mesenchymal Stem Cells

Primary hMSCs were cultured as plastic adherent cells to subconfluency, which took approximately 1 week (see Materials and methods). A characteristic feature of hMSCs is a $CD34^-$, $CD45^-$, $SH2^+$(CD105), and $SH3^+$(CD73) cell surface phenotype (Kobune *et al*, 2003). Both flattened and spindle-shaped cells can be recognized in the culture. Angiopoietin-1 gene-modified human mesenchymal stem cells showed similar flattened and spindle-shaped morphology. Flow cytometric analysis of the Ang-hMSCs (Figure 1B) was essentially identical to primary hMSCs (Figure 1A).

Detection of Immunoreactive Human Angiopoietin-1 and Quantitative Analysis *In Vitro*

Levels of Ang-1 in the supernatant of cultured hMSCs and Ang-hMSCs with different MOI levels were studied. Human mesenchymal stem cell transfected with AxCAhAng1-F/RGD (Ang-hMSC) at an MOI of 300, 1000, and 3000 pu/cell secreted Ang-1 at a rate of 40.75 ± 1.94, 130.08 ± 17.78, and 251.37 ± 10.31 ng/10^5 cells/48 h, respectively ($n = 4$). Non-transfected hMSC also produced Ang-1 protein (12.91 ± 0.093 ng/10^5 cells/48 h) ($n = 4$). These data are summarized in Figure 1C. The level of Ang-1 production from Ang-hMSC transfected at an MOI of 3000 pu/cell was approximately 20-fold greater than that observed in non-infected.

Characterization of Ischemic Lesion Size by Magnetic Resonance Image Analysis

An estimate of lesion size was obtained using *in vivo* MRI (see Materials and methods). The cells were intravenously delivered immediately after the 6 h MRI. Both T_2WI and DWI were carried. The reason is that the DWI is more useful for lesion volume detection in the acute infarction phase and the T_2WI is more important for later time points. Therefore,

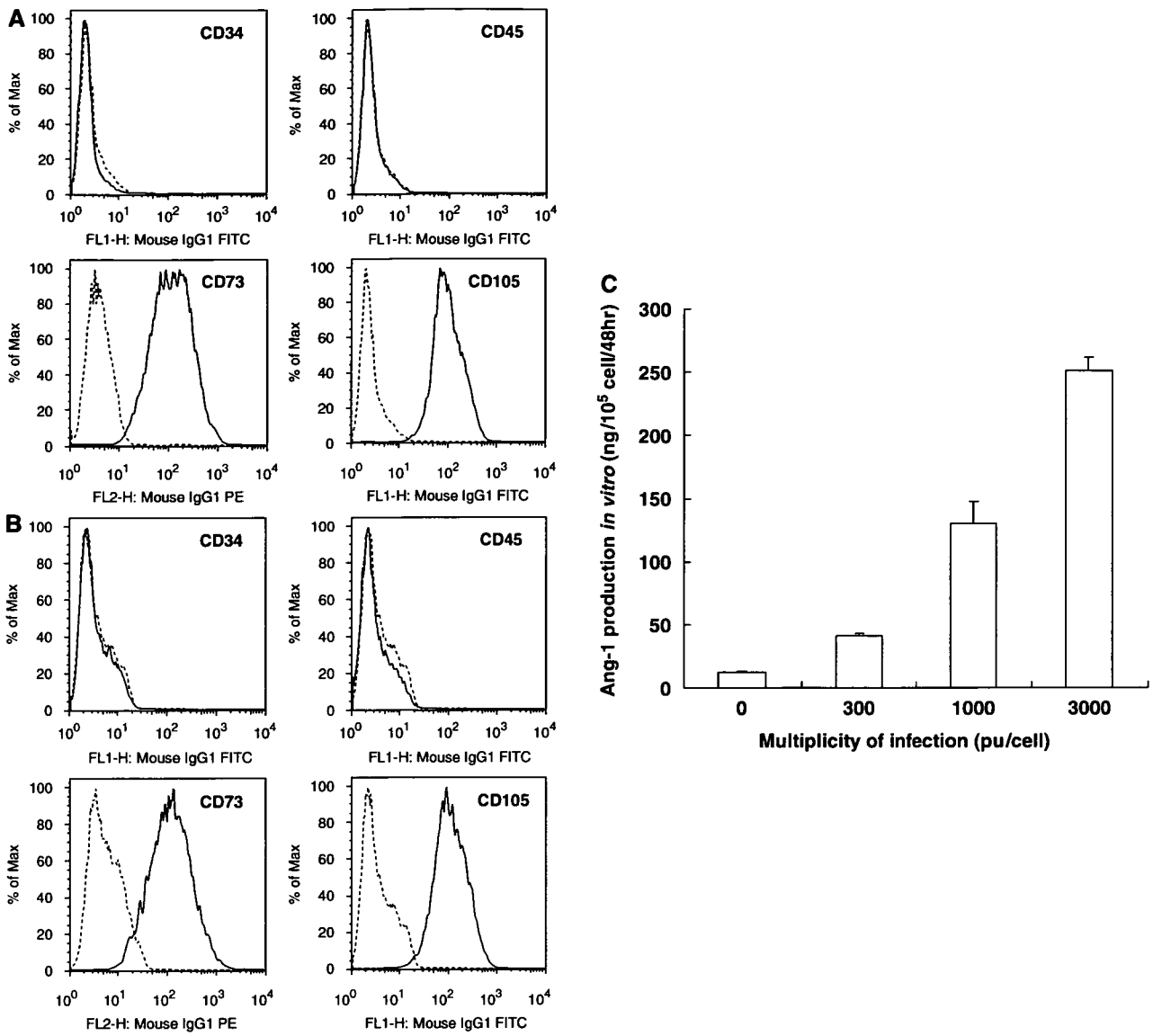

Figure 1 Flow cytometric analysis of surface antigen expression on primary hMSC (**A**) and Ang-hMSC (**B**). The cells were immunolabeled with FITC-conjugated monoclonal antibody specific for the indicated surface antigen. Dead cells were eliminated by forward and side scatter. Angiopoietin-1 production of hMSC, Ang-transfected hMSC were summarized (**C**). Levels of Ang-1 in the supernatant were shown.

DWI was used at only the time point of 6 h. Diffusion-weighted image and T_2WI are shown in Figures 2A and 2B, respectively. These coronal forebrain sections were obtained at the level of caudato-putamen complex. T2-weighted images obtained at 6 h, 1, 3, and 7 days are shown for control (medium) ($n = 15$), hMSC ($n = 10$), and Ang-hMSC-injected groups ($n = 8$) (Figure 2B). Note the reduction in density in lesions on the right side of the brains of the cell-treated groups at 7 days. Lesion volume (mm^3) was determined by analysis of high-intensity areas on serial images collected through the cerebrum (see Materials and methods).

To determine the efficacy of hMSCs or Ang-hMSCs transplantation in modulating the ischemic lesion volume, 1×10^6 cells were delivered intravenously at 6 h after MCAO, and animals were reimaged at 6, 24 h, 3, and 7 days later. In the sham control group, MRI-estimated lesion volume reached maximum at 3 days (Figure 2B-1–3) and gradually decreased at 7 days post-MCAO (Figure 2B-1–4). Although lesion volumes estimated 6 h after MCAO were the same among the three groups (Figures 2A and 2B) at 1, 3, and 7 days, lesion volume was less in both hMSC and Ang-hMSC groups as compared with control. The reduction in lesion volume showed no significant difference between the Ang-hMSC group and the hMSC group at 1, 3, and 7 days post-MCAO. These results are summarized in Figure 2C.

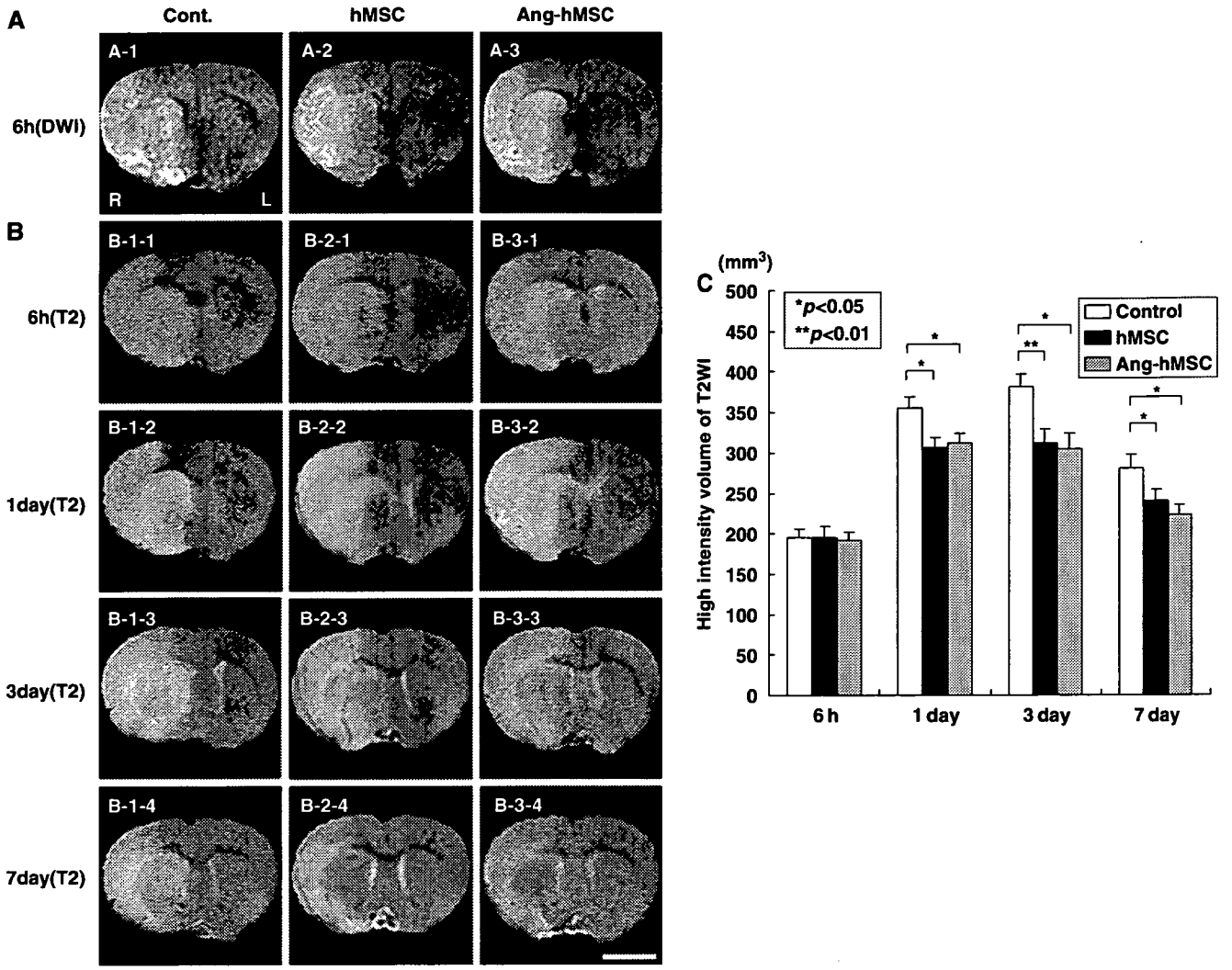

Figure 2 Evaluation of the ischemic lesion volume with DWIs and T_2WIs. Human mesenchymal stem cells or Ang-hMSCs were intravenously injected immediately after the initial MRI scanning (6 h after MCAO). Diffusion-weighted image obtained 6 h MCAO in medium-injected (**A-1**), hMSC-treated (**A-2**), and Ang-hMSC-treated group (**A-3**). T2-weighted images obtained 6 h, 1, 3, and 7 days MCAO in medium-injected (**B-1-1** to **-4**), hMSC-treated (**B-2-1** to -4), and Ang-hMSC-treated group (**B-3-1** to **-4**). Bar = 5 mm. (**C**) A summary of lesion volumes evaluated with MRI (T_2WI) were obtained 6 h, 1, 3, and 7 days after MCAO in rats treated with medium (control), hMSC, or Ang-hMSC.

Histological Determination of Infarction Volume

A second independent measure of infarction volume was performed. The brains were stained with TTC 7 days after MCAO (Figure 3). Normal brain (gray matter) tissue typically stains with TTC, but infarcted lesions show no or reduced staining (Bederson *et al*, 1986). 2,3,5-Triphenyltetrazolium chloride staining obtained 7 days after MCAO without cell transplantation is shown in Figure 3A. Note the reduced staining on the lesion side. Lesion volume was calculated by measuring the area of reduced TTC staining in the forebrain ($n = 5$) (see Materials and methods). As with MRI analysis there was a reduction in infarction volume with both hMSC ($n = 5$) (Figure 3B) and Ang-hMSC ($n = 5$) (Figure 3C) treatment. Intravenous delivery of 1×10^6 hMSCs and Ang-hMSCs resulted in very substantial reduction in lesion volume as estimated from TTC staining. The reduction in lesion volume was not significantly different between the Ang-hMSC group and the hMSC group at 7 days post-MCAO (Figure 3D).

Angiogenesis Induced by the Transplantation

To examine whether the administration of hMSCs and Ang-hMSCs induces angiogenesis, three-dimensional analysis of capillary vessels in the lesion was performed using Zeiss LSM5 PASCAL software. Figure 4A-1 shows the three-dimensional capillary image in the normal rat brain ($n = 4$). The capillary vascular volume in the boundary region after MCAO was increased in the hMSC-treated group ($n = 4$) (Figure 4A-3) compared with the medium-treated

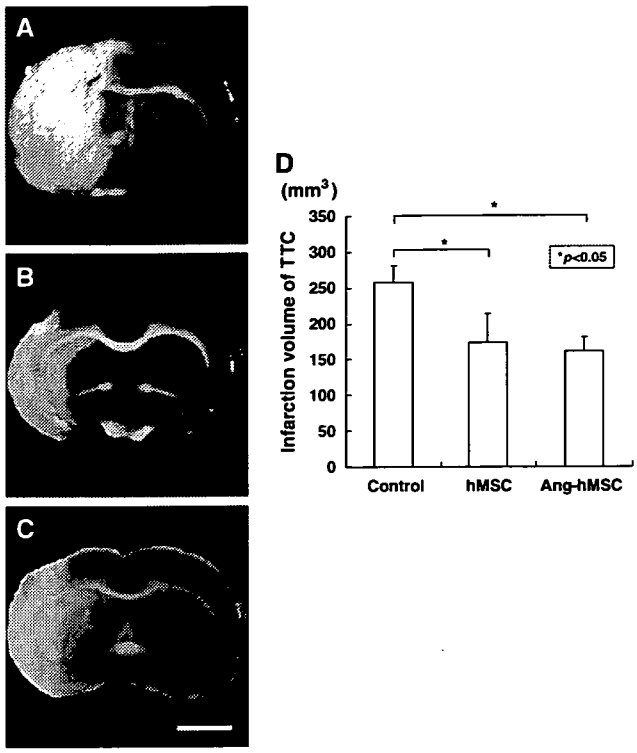

Figure 3 TTC Brain sections slices stained with TTC to visualize the ischemic lesions 7 days after MCAO. 2,3,5-Triphenyl tetrazolium chloride-stained brain slices from (**A**) medium-injected MCAO model rats, (**B**) following hMSC-treated, and (**C**) Ang-hMSC-treated groups. (**D**) Seven days after MCAO, there was a reduction in the lesion volume assayed using TTC staining for both hMSC and Ang-hMSC groups. Bar = 3 mm.

group ($n=4$) (Figure 4A-2), and the angiogenesis was greater in the Ang-hMSC-treated group ($n=4$) (Figure 4A–4).

The capillary vascular volume was expressed as a ratio by dividing that obtained from the ischemic hemisphere by that of the contralateral control hemisphere. At 7 days after MCAO, the ratio (ipsilateral/contralateral) was significantly higher in both the hMSC (0.17 ± 0.07; $P<0.05$) and the Ang-hMSC (0.46 ± 0.05; $P<0.001$)-treated groups as compared with the medium-treated group (0.13 ± 0.01). The ratio of the Ang-hMSC-treated group was significantly higher than the ratio of the hMSC-treated group. These results are summarized in Figure 4B. At 28 days after MCAO, the ratio (ipsilateral/contralateral) of Ang-hMSC-treated group (1.1 ± 0.29) was significantly higher than the ratio of hMSC-treated group (0.57 ± 0.12) and medium-treated group (0.26 ± 0.03). The ratio of the Ang-hMSC-treated group was significantly higher than the ratio of the hMSC-treated group. These results were summarized in Figure 4C.

LacZ-transfected hMSCs and Ang-hMSCs that had been intravenously administered (1.0×10^6 cells) 6 h after MCAO were identified *in vivo*. The LacZ-expressing MSCs were found primarily in the lesion. Note the abundance of β-gal-reaction product in and around the lesion, indicating that systemic delivery of the cells reached the lesion site (Figure 5A). There was a paucity of blue staining in the non-treated group.

Immunohistochemical studies were performed to identify LacZ-positive cells in and around the lesion zone in animals transplanted with LacZ-transfected hMSCs. The photomicrographs of hMSCs and Ang-hMSCs demonstrated a large number of LacZ-positive cells in and around the lesion (Figure 5B). Double staining was performed to show endothelial cell differentiation of LacZ-positive cells in the lesion zone in animals transplanted with LacZ-transfected Ang-hMSCs (Figure 5C). The vWF-positive cells in the boundary region 7 days after MCAO were increased in the hMSC-treated group ($n=4$) compared with the medium-treated group ($n=4$), which was the highest in the Ang-hMSC-treated group ($n=4$) (Figure 5D). Double-positive cells of vWF and LacZ were also increased in the Ang-hMSC-treated group compared with the hMSC-treated group (Figure 5E).

Dynamic Susceptibility Contrast-Enhanced Perfusion-Weighted Image

To assess regional cerebral blood flow, the PWI-derived parameter maps allowed further quantitative analysis for the hemodynamic changes of the lesions (see Materials and methods). Figures 6A–C shows images obtained at 6 h (row 1), 3 days (row 2), and 7 days (row 3). Control, hMSC- and Ang-hMSC-injected groups are in columns A, B, and C, respectively.

The four regions of interest (ROI) for the analysis are defined in Materials and methods. The severity of the lesion was greatest in ROI-1 and progressively less in ROI-2 through ROI-4. A rCBF ratio was calculated at each ROI from PWI obtained in the infarction hemisphere divided by that of the non-infarcted hemisphere. In ROI-1, the rCBF ratio of control, hMSC-treated, and Ang-hMSC-treated groups were similar and decreased to $<25\%$ at 6 h post-MCAO, and remained low at 3 and 7 days (Figure 6D). The rCBF ratio in ROI-2 of the three groups was similar at 6 h post MCAO. However, the rCBF ratio of both hMSC- and Ang-hMSC-treated groups was increased at 7 days after MCAO as compared with control (Figure 6E). The rCBF ratio in ROI-3 was similar for the three groups at 6 h, but again both hMSC- and Ang-hMSC-treated groups had a greater rCBF ratio at 3 and 7 days (Figure 6F). In ROI-4, the rCBF ratio slightly decreased in all groups at all time points, but not more than 10% (Figure 6G).

Functional Analysis

The maximum speed at which the rats could run on a motor-driven treadmill was recorded. Before

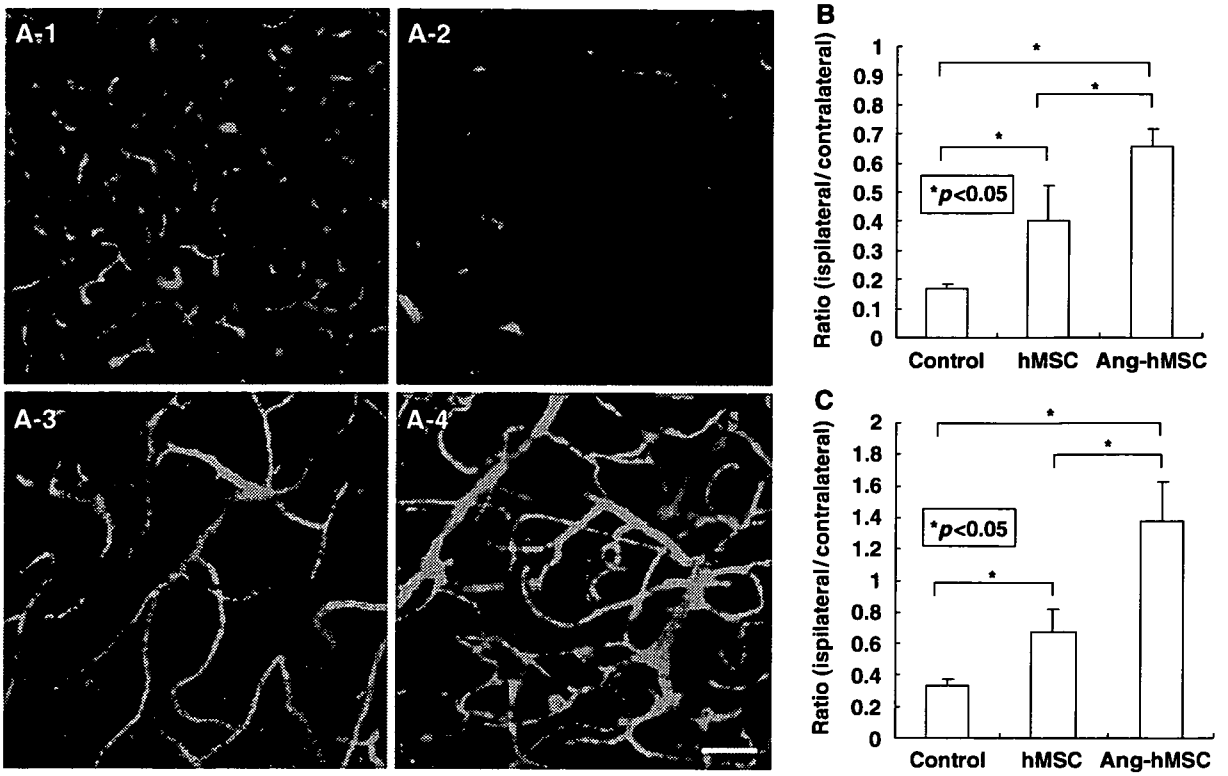

Figure 4 Seven and twenty-eight days after MCAO, the angiogenesis in boundary zone was analyzed using a three-dimensional analysis system. (**A-1**) Three-dimensional capillary image with systemically perfused FITC-dextran in the normal rat brain is shown. The total volume of the microvessels in the sampled lesion site decreased (**A-2**) 28 days after MCAO, but was greater in (**A-3**) the hMSC-treated group, and (**A-4**) the Ang-hMSC-treated group. These results are summarized in (**B**) (7 days after MCAO) and (**C**) (28 days after MCAO). The ratio (ispilateral/contralateral) was significantly higher in both the hMSC- and the Ang-hMSC-treated groups as compared with the medium-treated group. Also the ratio of the Ang-hMSC-treated group was significantly higher than the ratio of the hMSC-treated group. Bar = 150 μm.

MCAO, there was no significant difference among control ($n=27$), hMSC-treated ($n=21$), and Ang-hMSC-treated groups ($n=19$) (Figure 7); and at 6 h post-MCAO there was comparable impairment among three groups. Twenty-four hours after MCAO maximum velocity on the treadmill test was at its maximum deficit. An increase in maximum velocity was observed for the Ang-hMSC group at 24 h. Both hMSC and Ang-hMSC groups had greater maximum velocity from 3 to 7 days than sham control, but the Ang-hMSC group attained a higher velocity than the hMSC group. These results are summarized in Figure 7.

Discussion

This study demonstrates that intravenous infusion of either hMSCs or Ang-hMSCs 6 h after permanent MCAO in the rat results in reduction in infarction volume, an induce in angiogenesis, and improvement in behavioral performance. These results are consistent with previous studies showing beneficial effects of bone marrow cell transplantation in experimental cerebral ischemic models (Chen *et al*, 2001; Iihoshi *et al*, 2004; Nomura *et al*, 2005; Honma *et al*, 2006; Horita *et al*, 2006; Kim *et al*, 2006; Liu *et al*, 2006; Ukai *et al*, 2007). Both hMSCs and Ang-hMSCs comparably reduced gross lesion volume as assayed with MRI and histology. Angiogenesis and rCBF were increased after infusion of either cell type, but were greater in small border areas after Ang-hMSC infusion. Functional recovery was also improved for both cell types, but modestly greater in the Ang-hMSC group. Thus, Ang-hMSCs do not effect lesion volume any more than hMSCs, but may facilitate small pockets of regional neovascularization and modest augumented functional recovery.

Both VEGF and Ang-1 play important roles in forming new vessels. Vascular endothelial growth factor has a role in enlarging small vessels (Pettersson *et al*, 2000). Although VEGF can initiate vessel formation, on its own it promotes formation of leaky, immature, and unstable vessels. Such destabilized vessels would be prone to regression in the absence of associated growth factors. In contrast, Ang-1 induces vessel sprouting and branching (Davis *et al*, 1996; Koblizek *et al*, 1998), and seemingly further stabilizes and protects the adult vasculature, making

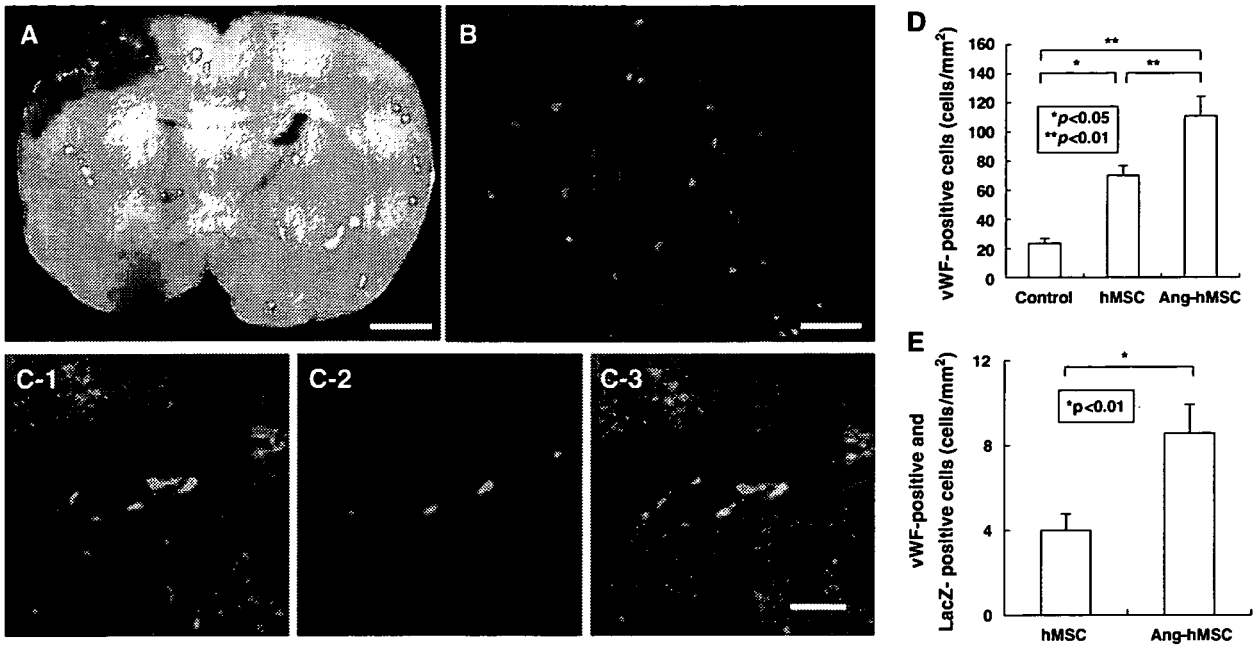

Figure 5 Intravenously-administered Ang-hMSCs accumulated in and around the ischemic lesion hemisphere. Angiopoietin-1 gene-modified human mesenchymal stem cells were transfected with the reporter gene LacZ. (**A**) Transplanted LacZ-positive Ang-hMSCs (blue cells) were present in the ischemic lesion. (**B**) Confocal images demonstrating a large number of LacZ-positive cells in the lesion hemisphere. Ang-hMSCs differentiated into the endothelial lineage. (**C-1** and **C-2**) Confocal images show the transplanted cells (**C-2**: LacZ in red) and endothelial cells (**C-1**: vWF in green). Panel **C-3** confirms the co-labeling of LacZ/vWF in the cells. The cell density of vWF-positive cells are shown in **D**. Panel **E** demonstrates the cell density of vWF-positive cells co-localized with LacZ. Bar: (**A**)—3 mm; (**B**)—150 μm; and (**C**)—50 μm.

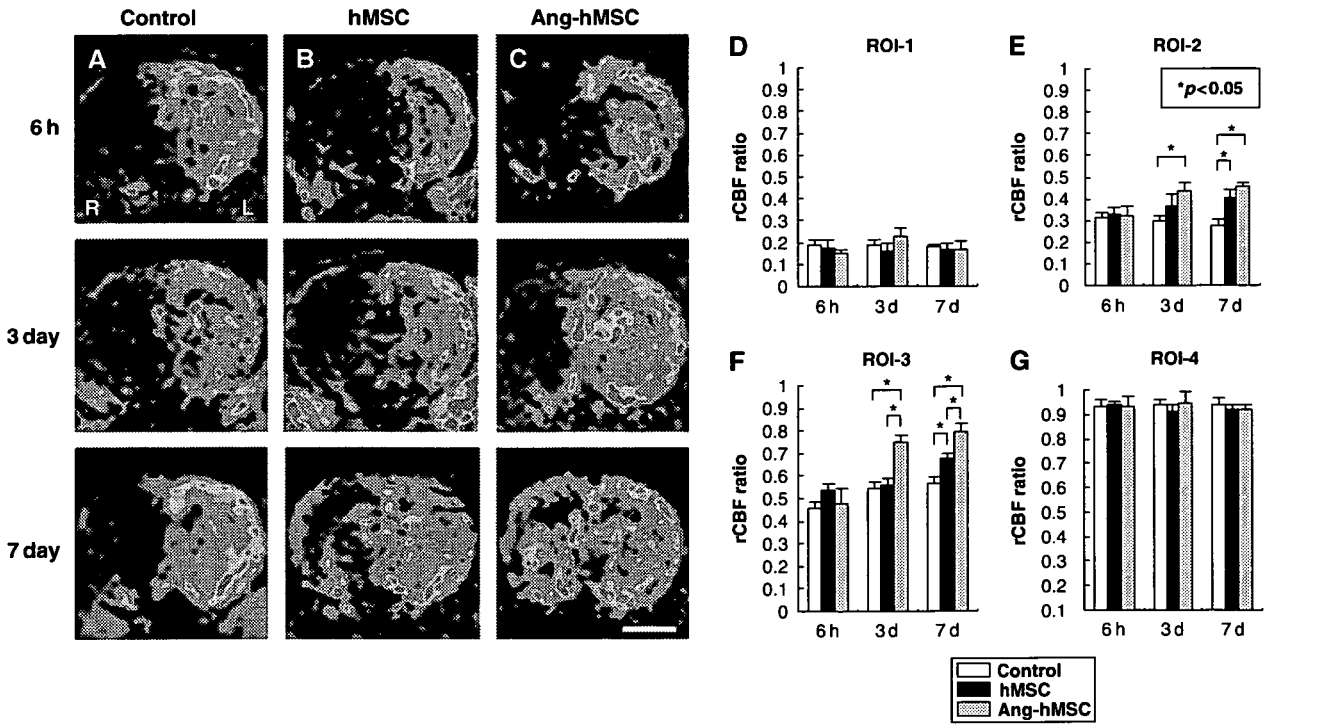

Figure 6 Evaluation of hemodynamic state (rCBF maps) with PWIs. Human mesenchymal stem cells or Ang-hMSCs were intravenously injected immediately after the initial MRI scanning (6 h after MCAO). Images obtained 6 h, 3, and 7 days MCAO in (**A**) medium-injected, (**B**) hMSC-treated, and (**C**) Ang-hMSC-treated group. (**D–G**) Summary of rCBF evaluated with PWI in each groups. (**D**) ROI-1, (**E**) ROI-2, (**F**) ROI-3, and (**G**) ROI-4. Regional cerebral blood flow ratio (ischemic lesion/contralateral lesion) at 6 h, 3, and 7 days after MCAO are summarized in D–G. Bar = 3 mm, $*P < 0.05$.